

bond, depicted in the -2.6 to -2.2 Å region of Figure 2 (negative sign merely represents P-O₃ translation). The resulting structure is very similar, by symmetry, to the stereoelectronically favored P-O₂ transition state geometry shown in Figure 1b.

We next explored the energy profile for the rotation of the equatorial P-O₃ bond in oxyphosphorane **3a** to examine the stereoelectronic effects in the intermediate and the transition state. In Figure 3, the rotational profile (top) for the axial P-O₂ bond breaking step is plotted with the rotational profile (bottom) of the metastable intermediate **3a**.^{8,10} The rotational energy profile for the axial P-O₂ bond breaking step was calculated with the fixed P-O₂ bond length of 2.173 Å, which is the calculated value at the P-O₂ bond breaking transition state (Figure 1b). In the rotational energy profile for the P-O₂ bond breaking step, one of the two metastable-state local minima at a $\tau(\text{O}_2\text{PO}_3\text{Me})$ of around 130°, corresponding to the stereoelectronically unfavorable P-O bond breaking pathway, has completely disappeared. This is in accord with P-O₃ bond rotation at the increased P-O₃ bond length of 2.2 Å (see Figure 2).

The energy profiles shown in Figures 2 and 3 indicate that a stereoelectronically unfavorable transition state with only one negative eigenvalue should be unattainable: Even though the energy increases with P-O₃ bond lengthening in the -2.0 to -2.2 Å region (Figure 2), the energy well at a $\tau(\text{O}_2\text{PO}_3\text{Me})$ of around 130° has already disappeared when the P-O₂ bond length is 2.173 Å (Figure 3).¹¹⁻¹³ It is also noteworthy that the metastable-state stereoelectronic effect is ca. 2 kcal mol⁻¹ as evidenced from the bottom profile connecting open squares in Figure 3; on the other hand, the stereoelectronic effect at the transition state is at least 6 kcal mol⁻¹ as extrapolated at the point of $\tau(\text{O}_2\text{PO}_3\text{Me}) = 130^\circ$ and P-O₃ = 2.173 Å of the top profile. In reality, a transition-state stereoelectronic effect must be much larger than 6 kcal mol⁻¹, because the putative transition state for the P-O₃ bond cleavage step would be expected to occur much later at P-O₃ > 2.7 Å if the stereoelectronically unfavorable transition state could have existed as in **2a**. In fact, under C₃ symmetry, the energy difference between the stereoelectronically favorable and unfavorable transition states in **3b** was calculated to be ca. 29 kcal mol⁻¹.¹² These results support earlier emphasis that the kinetic stereoelectronic effect and the α -effect are largely transition-state phenomena.¹⁴

Since the present results suggest that the stereoelectronically¹⁵ disfavored axial P-O bond cleavage and formation should not occur in the acyclic oxyphosphorane system, the equatorial P-O₃ bond rotation during the reaction must be essential for the axial attack and axial departure (in-line) mechanisms in the base-catalyzed acyclic phosphate ester methanolysis. The relative energies of

the transition states for the axial P-O bond cleavage and for the equatorial P-O bond rotation are calculated to be comparable, and both have activation energies of less than 2 kcal mol⁻¹ with respect to the metastable intermediate **3a**.¹⁶ Thus, all events consisting of attack, rotation, and cleavage after rotation turn out to be only partially rate determining.¹⁷

The recent report by Lim and Karplus⁶ suggesting the nonexistence of the dianionic intermediate of cyclic oxyphosphorane system **2b** is in contrast to the acyclic oxyphosphorane system **3a** presented here. The cause for this discrepancy does not seem to arise from the cyclic nature of **2b**, since our calculations at the 3-21G* level of theory also support the existence of the dianionic intermediate **2a**.¹³ Instead, the contrast can be reconciled by the difference of the axial substituents (OH vs OMe). Bigger substituents probably better delocalize the dianionic charges and stabilize the intermediates in the gas phase.¹⁸ Consequently, in the case of Karplus's system, less stable **2b** abolished the stereoelectronically favorable P-O₂ bond breaking transition state, leaving only the P-O₃ bond breaking transition state.

(16) The energy well around the metastable intermediate **3a** remains after zero point energy correction at the three stationary points optimized at the 3-21G* level: the metastable intermediate and the transition state for the axial P-O bond breaking and for the equatorial P-O bond rotation. The well depth is calculated to be 0.54 kcal mol⁻¹ at the 3-21G* level with zero-point energy included.

(17) Consequently, for the lowest energy pathway of methoxide attack on dimethyl phosphate monoanion: (i) MeO⁻ attacks phosphorus following the right half profile of Figure 2 (P-O₂ bond length of 2.8-1.9 Å region); (ii) the equatorial MeO group rotates following the bottom profile of Figure 3 (from a $\tau(\text{O}_2\text{PO}_3\text{Me})$ value of 50.1° to 129.9°, corresponding to two local minima of the metastable state); and (iii) MeO⁻ leaves following the reversed pathway of (i) because of the structural symmetry.

(18) Under C₁ symmetry, the oxyphosphorane species **3b** does not exist as a stable intermediate.¹² However, recent work by Karplus et al. shows that, for the attack of OH⁻ on dimethyl phosphate monoanion, an intermediate does exist at the 3-21G* and 3-21+G* level, and they obtained an energy profile like Figure 2 of this study.²⁰ Moreover, our unpublished results on *monoanionic 2a* indicate that it is a much more stable intermediate than *dianionic 2a*. These results are in accord with our interpretation of delocalized charges. Furthermore, solvation should stabilize a dianionic intermediate relative to two monoanionic reactants (see also the conclusion of ref 13).

(19) Taira, K.; Uchamaru, T.; Storer, J. W.; Tanabe, K.; Nishikawa, S., manuscript in preparation.

(20) Dejaeger, A.; Lim, C.; Karplus, M. *J. Am. Chem. Soc.*, following paper in this issue.

Dianionic Pentacoordinate Species in the Base-Catalyzed Hydrolysis of Ethylene and Dimethyl Phosphate[†]

A. Dejaeger,[‡] C. Lim,[§] and M. Karplus*

Department of Chemistry, Harvard University
Cambridge, Massachusetts 02138

Received February 4, 1991

The nature of the pentacoordinate species involved in the hydrolysis of phosphate esters in enzymes and aqueous solution is still unclear. Recently, we reported gas phase ab initio calculations¹ which showed that there is no dianionic pentacoordinate intermediate along the gas-phase reaction path for the basic hydrolysis of ethylene phosphate, a model for the rate-determining step in the enzymatic hydrolysis of RNA by bovine ribonuclease A.² Specifically, in the nucleophilic attack by OH⁻ on the cyclic ester, ethylene phosphate (i.e., OH⁻ + (CH₂O)₂PO₂⁻ → HOCH₂CH₂OPO₃²⁻), a pentacoordinate dianionic species is a transition state but not an intermediate at the Hartree-Fock 3-21G* or 3-21+G* ab initio level,³ even though STO-3G cal-

(10) The rotational energy profiles for the metastable state and for the P-O₂ bond breaking step were explored starting from the local-minimum geometry of the metastable state (Figure 1a) and from the P-O₂ transition-state geometry (Figure 1b). Each point comprising the energy profiles was obtained by the geometry optimization at each torsional angle.

(11) A P-O₃ transition state for **3b** with the P-O₃ bond length of 3 Å was found at 3-21G* level under C₁ symmetry restricted conditions,¹² corresponding to unfavorable P-O₃ bond breaking in this study. Moreover, because of the unique cyclic nature of **2a**, its 3-21G* transition state for stereoelectronically unfavorable exocyclic P-O₃ bond cleavage has been located, without assuming any symmetry, at the P-O₃ bond length of 2.728 Å.¹⁹ Note that, in terms of the orientation of lone-pair electrons on O₃, the P-O₃ bond in **2a** is equivalent to the P-O₃ bond in **3a**. Our results presented here indicate that the stereoelectronically unfavorable transition state occurring with such a long bond distance should not be possible in the acyclic system.

(12) Taira, K.; Uchamaru, T.; Tanabe, K.; Uebayasi, M.; Nishikawa, S., *Nucleic Acids Res.*, in press.

(13) Storer, J. W.; Uchamaru, T.; Tanabe, K.; Uebayasi, M.; Nishikawa, S.; Taira, K. *J. Am. Chem. Soc.*, in press.

(14) Taira, K.; Gorenstein, D. G. *J. Am. Chem. Soc.* **1984**, *106*, 7825-7831.

(15) Note that the energy profiles in Figure 3 can be explained by the optimal orbital interactions between nonbonding lone pair orbitals on equatorial oxygen and antibonding σ^* orbitals of axial P-O bonds.⁵ We call this reactivity dependence on the orientation of lone-pair electrons a "stereoelectronic effect", although we do not know the exact origin of the effect as to whether it is due to orbital mixing or other factors, since the overlap populations and Mulliken charges calculated for oxyphosphorane species **3a** are not necessarily in accord with the orbital mixing interpretation.

[†]Supported in part by a grant from the National Science Foundation.

[‡]Supported by the Belgian National Fund for Scientific Research.

[§]Present address: Department of Medical Genetics, Medical Science Building, University of Toronto, Toronto, Ontario, M5S 1A8 Canada.

(1) Lim, C.; Karplus, M. *J. Am. Chem. Soc.* **1990**, *112*, 5872.

(2) Fersht, A. *Enzyme Structure and Mechanism*; W. H. Freeman & Co.: New York, 1985.

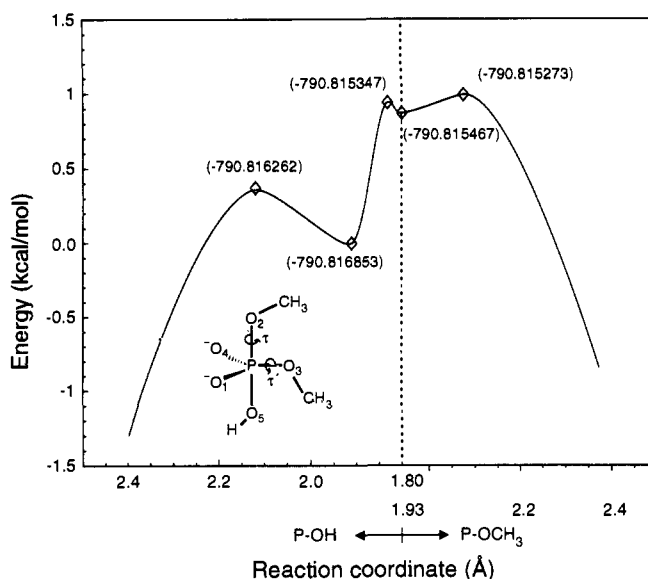


Figure 1. The reaction path for $\text{OH}^- + (\text{CH}_3\text{O})_2\text{PO}_2^- \rightarrow (\text{CH}_3\text{O})(\text{O}-\text{H})\text{PO}_2^- + \text{OCH}_3^-$ at the 3-21+G* level; the P-O5 (P-OH) distance is used as the reaction coordinate for the first part of the reaction and the P-O2 (P-OCH₃) distance for the second part of the reaction; the gauche region for the dihedral angles τ and τ' (see drawing for definitions) is defined as $60 \pm 30^\circ$ and the trans region as $180 \pm 40^\circ$. The gauche (τ), trans (τ') intermediate has been chosen as the zero of energy. The five stationary points shown in the figure have their Hartree-Fock 3-21+G* energies listed in parentheses. They were fully optimized except for methyl groups which were constrained so that the C-H bonds are the same length and that two H-C-H angles are equal. To determine the form of the reaction profile curve (solid line), other points (not shown) were calculated with partial optimization and some additional constraints.

calculations yield a pentacoordinate intermediate with a barrier of 8.3 kcal/mol to unimolecular ring opening. To determine the generality of this result, we have done *ab initio* calculations for the attack of OH^- on the acyclic ester, dimethyl phosphate. Again, the STO-3G calculation shows the existence of a pentacoordinate intermediate,⁴ but there also exist in this species, unlike the cyclic species, intermediates at the 3-21G* and 3-21+G* level. However, the transition state for breaking the axial P-OCH₃ bond is only 0.12 kcal/mol above the intermediate at the 3-21+G* level, in contrast to the STO-3G value of 3.6 kcal/mol; Gorenstein et al.⁴ obtained an STO-3G barrier of 12 kcal/mol. Further, because of the greater conformational freedom of the acyclic ester, the reaction path for OH^- addition and OCH_3^- elimination has an interesting complexity. The gas-phase potential surface at the Hartree-Fock 3-21+G* level shows two shallow pentacoordinate intermediates and three transition states with the dihedral angle for rotation around the P-O3 bond strongly coupled to the reaction coordinate (see Figure 1 for definitions; in what follows, the first dihedral angle refers to τ and the second to τ'). As the OH^- approaches, the lowest energy species is gauche, trans. It remains so at the first transition state (P-O5, 2.11 Å; P-O2, 1.76 Å; τ , 68.9°; τ' , 145.8°) and at the first intermediate (P-O5, 1.91 Å; P-O2, 1.80 Å; τ , 69.2°; τ' , 145.5°). As the OH^- group approaches more closely, the equatorial OCH_3^- rotates away from the attacking OH^- . The reaction goes through a second transition state that is gauche, gauche (P-O5, 1.83 Å; P-O2, 1.88 Å; τ , 71.0°; τ' , 85.0°). The second intermediate is also gauche, gauche (P-O5, 1.80 Å; P-O2, 1.93 Å; τ , 73.1°; τ' , 69.4°), as is the final transition state (P-O5, 1.77 Å; P-O2, 2.07 Å; τ , 75.6°; τ' , 63.8°).

(3) The notation 3-21G* implies a split valence basis set with 3d functions on phosphorus; 3-21+G* also includes a diffuse sp function on non-hydrogen atoms; no polarization functions are used on atoms other than phosphorus. For a more detailed description of the basis sets, see: Hehre, W. J.; Radom, L.; Schleyer, P. v. R.; Pople, J. A. *Ab initio Molecular Orbital Theory*; Wiley: New York, 1986.

(4) Gorenstein, D. A.; Luxon, B. A.; Findley, T. B. *J. Am. Chem. Soc.* **1979**, *101*, 5869.

Table I. Basis Set Superposition Error for OCH_3^- ^a

P-OCH ₃ (Å)	STO-3G	3-21G*	3-21+G*
∞	0.0	0.0	0.0
5.0	0.0	0.0	-0.3
3.5	-0.4	-5.6	-0.7
2.5	-17.1	-17.5	-1.8
1.955	-49.2	-24.4	-3.2
1.5	-75.2	-32.9	-6.0
1.0	-97.1	-44.2	-10.1

^a Values relative to isolated OCH_3^- . The basis set superposition error was calculated by the counterpoise method of Boys and Bernardi;⁸ units: kcal/mol. The ghost functions added were those of the $[\text{P}(\text{O}-\text{H})\text{O}_2\text{OCH}_3]^-$ moiety of the reaction complex in the gauche (τ), gauche (τ') conformation.

The change in geometry found in the dimethyl phosphate attack by OH^- (i.e., gauche, trans for OH^- addition and gauche, gauche for OCH_3^- elimination) is consistent with stereoelectronic arguments.⁵ However, further tests are needed to determine if stereoelectronic effects cause the conformational preference or if they are merely correlated with it, as has been suggested.^{6,7}

To examine the origin of the large difference between the potential energy surface obtained from STO-3G and 3-21+G* calculations, we have used the counterpoise method⁸ to estimate the basis set superposition error (BSSE) of the methoxide displacement reaction profile (Table I). The difference between the STO-3G, 3-21G*, and 3-21+G* results is striking and indicative of the origin of the incorrect potential surface obtained from STO-3G calculations; i.e., the STO-3G basis set artificially stabilizes the reaction complex as the P-O2 distance decreases and creates a well on the potential energy surface. This behavior is in accord with studies of anion-water complexes, where the superposition error for minimal basis sets was of the order of magnitude of the interaction energy and the addition of diffuse functions to the basis set led to significant improvements in the interaction energy curves.⁹

The present calculations lead to the perhaps not surprising conclusion that the reaction path for the hydrolysis of phosphate esters can be rather complex, even in the gas phase. The results at the 3-21+G* level for the acyclic and cyclic species, as well as the 3-21G* results for attack by OCH_3^- rather than OH^- (see accompanying communication by Uchimaru et al.; C. Lim, unpublished work) show that dianionic pentacoordinate intermediates either do not exist or are only marginally stable in the gas phase; stable intermediates (with barrier heights of several kilocalories/mole for dissociation) appear to be an artifact of the STO-3G basis set, at least in part due to BSSE. Further, when zero-point energy is included, some of the intermediates on the potential surface are modified and may disappear; e.g., the zero point energy correction is 70.1 kcal/mol for the gauche, trans intermediate relative to 69.7 kcal/mol for the next transition state. The intermediates, which have well depths on the order of $k_B T$, are unlikely to be kinetically significant. Thus, the results reported here are in accord with the interpretation given previously¹ of the difference between the dianionic and monoanionic species; i.e., in contrast to the dianionic species, monoanionic species are expected to have intermediates with deeper wells in the gas phase.

Improvements in the *ab initio* calculations using larger basis sets and including electron correlation would be desirable, though costly,¹⁰ electron correlation is known to be of particular importance in hydrogen-bonded¹¹ and dianionic species.¹² Most

(5) Gorenstein, D. G. *Chem. Rev.* **1987**, *87*, 1047.

(6) Thatcher, G. R. J.; Kluger, R. *Adv. Phys. Org. Chem.* **1989**, *25*, 99.

(7) Sinnott, M. *Adv. Phys. Org. Chem.* **1988**, *24*, 113.

(8) Boys, S. F.; Bernardi, F. *Mol. Phys.* **1970**, *19*, 553.

(9) Alagona, G.; Ghio, C.; Latajka, Z.; Tomasi, J. *J. Phys. Chem.* **1990**, *94*, 2267. Sordo, J. A.; Sordo, T. L.; Fernandez, G. M.; Gomperts, R.; Chin, S.; Clementi, E. *J. Chem. Phys.* **1989**, *90*, 6361.

(10) For ethylene phosphate, an MP2/6-31+G* single-point calculation for the reactants and the transition state increased the activation barrier by 3 kcal/mol.

(11) Frisch, M. J.; Del Bene, J. E.; Binkley, J. S.; Schaeffer, H. F., III. *J. Chem. Phys.* **1986**, *84*, 2279.

(12) Simons, J.; Jordan, K. D. *Chem. Rev.* **1987**, *87*, 535.

important are calculations to determine how the reaction profile is modified by solvation. It is well recognized that the behavior of ionic species, in particular, can be very different in the gas phase and solution, so that care is required in extrapolating from the former to the latter. In the present system, there are important differences between the gas-phase calculations and experimental solution results; e.g., the enthalpy of activation for the basic hydrolysis of dimethyl phosphate is estimated to be 28 kcal/mol,¹³ in contrast to the gas-phase 3-21 + G* result of about 90 kcal/mol. Use of a Born type model suggests that a dianionic intermediate will be stabilized significantly more than two monoanionic reactants since the solvation free energy and enthalpy depend quadratically on the charge of the ion.¹⁴ Simulations along the reaction path to provide more quantitative evaluations of the relative solvation free energies of the different species are in progress. Their comparison with empirical rules for phosphate ester hydrolysis^{6,15,16} will be of great interest.

Acknowledgment. We thank K. Taira for providing results prior to publication and for delaying his manuscript so that the two papers would be published together. Most of the calculations were done at the Pittsburgh Supercomputing Center.

- (13) Haake, D. C. Ph.D. Thesis, Harvard University, 1960.
 (14) Yu, H.-A.; Roux, B.; Karplus, M. *J. Chem. Phys.* **1990**, *92*, 5020.
 (15) Westheimer, F. M. *Acc. Chem. Res.* **1968**, *1*, 70.
 (16) Holmes, R. R. *J. Am. Chem. Soc.* **1978**, *100*, 433.

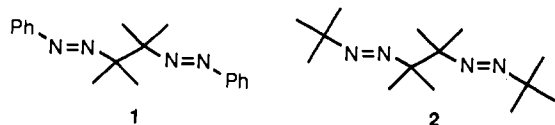
Formation of α - and β -Azo Radicals by C-C and C-N Homolysis of Vicinal Bisazoalkanes

Paul S. Engel,* Yanqiu Chen, and Chengrong Wang

Department of Chemistry, Rice University
 P.O. Box 1892, Houston, Texas 77251

Received January 23, 1991

While azoalkanes are well-known precursors of carbon-centered radicals,^{1,2} the azo group as a radical-stabilizing substituent³ has received little attention.⁴ Even less is known about azoalkanes whose β -carbon bears a radical center;⁵ in fact, such species could lose nitrogen so rapidly as to be undetectable. Our longstanding interest in azoalkanes and more recently in bisazoalkanes⁶ prompted us to examine the thermolysis of compounds 1 and 2.⁷



Although C-N bond cleavage is the normal decomposition mode of azoalkanes,¹ the work of Wintner⁸ and others⁹ demonstrates

- (1) Engel, P. S. *Chem. Rev.* **1980**, *80*, 42.
 (2) Adam, W.; De Lucchi, O. *Angew. Chem., Int. Ed. Engl.* **1980**, *19*, 762.
 (3) Viehe, H. G.; Janousek, Z.; Merenyi, R., Eds. *Substituent Effects in Radical Chemistry*; NATO ASI Series C, Vol. 189; D. Reidel Publ. Co.: Dordrecht, Holland, 1986.
 (4) McKee, M. L. *J. Am. Chem. Soc.* **1990**, *112*, 7957. Tomasic, Z. A.; Scuseria, G. E. *Chem. Phys. Lett.* **1990**, *170*, 21.
 (5) Malament, D. S.; McBride, J. M. *J. Am. Chem. Soc.* **1970**, *92*, 4586.
 (6) Chen, Y.; Engel, P. S. 42nd Southwest Regional Meeting of the American Chemical Society, Houston, TX, Nov 19, 1986; paper 410. Engel, P. S.; Chen, Y. *Abstracts of Papers*, 194th National Meeting of the American Chemical Society, New Orleans, LA; American Chemical Society: Washington, DC, 1987; ORGN 175. Engel, P. S.; Chen, Y. *Abstracts of Papers*, 197th National Meeting of the American Chemical Society, Dallas, TX; American Chemical Society: Washington, DC, 1989; ORGN 70.
 (7) Spectral data for 1: ¹H NMR (90 MHz, C₆D₆) δ 1.51 (s, 12 H), 7.80 (m, 6 H), 7.10 (m, 4 H); ¹³C NMR (22.5 MHz, C₆D₆) δ 152.82, 130.28, 129.58, 75.32, 21.55; UV (hexane) λ_{max} = 410 nm, ϵ = 258; MS (30 eV) *m/e* (relative abundance) 41(31), 51(33), 69(17), 77(100), 105(86), 147(1), 148(1), 182(2), 189(2), 210(1), 294(1). Anal. Calcd for C₁₈H₂₂N₄: 294.1844. Found: 294.1845. Spectral data for 2: ¹H NMR (90 MHz, C₆D₆) δ 1.21 (s, 18 H), 1.32 (s, 12 H); ¹³C NMR (22.5 MHz, C₆D₆) δ 73.15, 66.87, 26.92, 21.01; UV (hexane) λ_{max} = 372 nm, ϵ = 30. Anal. Calcd for C₁₄H₂₀N₄: 254.2470. Found: 254.2468.

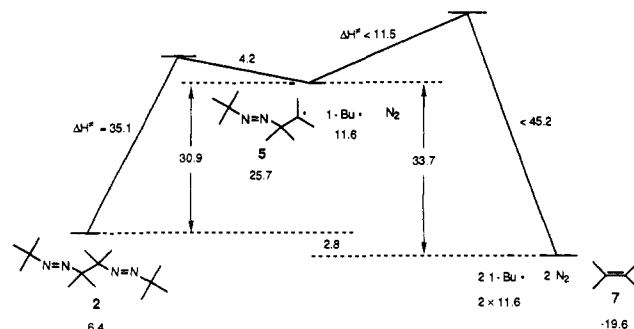
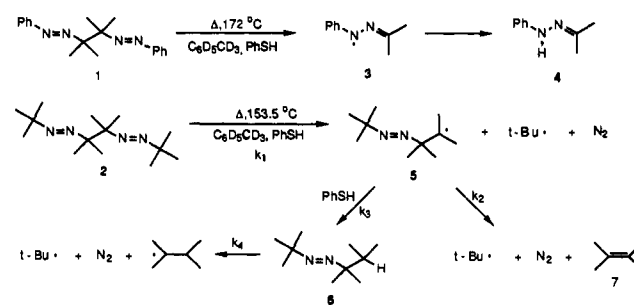


Figure 1. Enthalpy diagram for stepwise fragmentation of 2. Calculated heats of formation (kcal/mol) are shown below each species. The strain energies of 2 and 5 are estimated while ΔH_f of *t*-Bu• is from ref 16.

that C-C bond homolysis can also occur. Unfortunately, the vicinal bisazoalkanes studied to date⁸ are complicated by possible tautomerization and by α -aryl groups that contribute in an unknown way to the lability of the adjacent bonds.

We report here that thermolysis of 1 leads exclusively to cleavage of the central C-C bond while 2 undergoes only C-N homolysis via a short-lived β -azo radical. This remarkably different behavior is most readily seen in the nitrogen yield, which is <0.5% for 1 at 171.7 °C and 199% for 2 at 156.6 °C. In the presence of thiophenol, 1 affords exclusively acetone phenylhydrazone (4) and diphenyl disulfide while 2 yields isobutane, tetramethylethylene (7), and diphenyl disulfide.



Thermolysis kinetics were studied for both vicinal bisazoalkanes. The NMR spectrum of degassed 1 with added PhSH in C₆D₆ was monitored with time over the temperature range 133.3–158.1 °C, leading to the activation parameters $\Delta H^\ddagger = 30.2 \pm 0.6$ kcal/mol, $\Delta S^\ddagger = -4.3 \pm 1.3$ eu, and $\Delta G^\ddagger(150^\circ\text{C}) = 32.0$ kcal/mol.¹⁰ UV spectroscopy was used to monitor the disappearance of 2 in toluene over the temperature range 153.5–180.0 °C, providing the activation parameters $\Delta H^\ddagger = 35.1 \pm 0.9$ kcal/mol, $\Delta S^\ddagger = 2.7 \pm 2.2$ eu, and $\Delta G^\ddagger(150^\circ\text{C}) = 34.0$ kcal/mol. The 2.0 kcal/mol greater stability of 2 than 1 will be rationalized below.

Similar to the longstanding controversy about stepwise versus simultaneous bond cleavage of simple azoalkanes,¹¹ the question arises whether 2 breaks four C-N bonds at once or whether β -azo radical 5 is the reaction intermediate. We ignore the possible intervention of *tert*-alkyldiazenyl radicals, whose lifetime is expected to be less than 0.5 ps.¹² In an attempt to trap 5, a sample

- (8) (a) Wintner, C.; Wiecko, J. *Tetrahedron Lett.* **1969**, 1595. (b) Woodward, R. B.; Wintner, C. *Tetrahedron Lett.* **1969**, 2693. (c) Woodward, R. B.; Wintner, C. *Tetrahedron Lett.* **1969**, 2697 and references cited therein.
 (9) (a) Chang, M. H.; Dougherty, D. A. *J. Am. Chem. Soc.* **1982**, *104*, 2333 and references cited therein. (b) McNeil, D. W.; Kent, M. E.; Hedaya, E.; D'Angelo, P. F.; Schissel, P. O. *J. Am. Chem. Soc.* **1971**, *93*, 3817. (c) Adam, W.; Dörr, M.; Hill, K.; Peters, E.-M.; Peters, K.; von Schnering, H. G. *J. Org. Chem.* **1985**, *50*, 587 and references cited therein.
 (10) The thermolysis rates of 1, 2, and 6 were determined at four or five temperatures. In each kinetic run, the NMR relative peak area or UV absorbance was measured at 7–10 elapsed times. The oil-bath temperature was regulated to ± 0.01 °C and was measured to nearly the same precision with a platinum thermometer.
 (11) Neuman, R. C.; Grow, R. H.; Binegar, G. A.; Gunderson, H. J. *J. Org. Chem.* **1990**, *55*, 2682 and references cited therein.
 (12) Engel, P. S.; Gerth, D. B. *J. Am. Chem. Soc.* **1983**, *105*, 6849.